

Single Spin Asymmetries of Identified Hadrons in Polarized $p+p$ at $\sqrt{s} = 62.4$ and 200 GeV

J.H. Lee and F. Videbæk (For the BRAHMS Collaboration)

*Physics Department, Brookhaven National Laboratory
Upton, NY 11973, USA*

Abstract. Measurements of x_F -dependent single spin asymmetries of identified charged hadrons, π^\pm , K^\pm , p , and \bar{p} , from transversely polarized proton collisions at $\sqrt{s} = 200$ and 62.4 GeV at RHIC are presented. The energy and flavor dependent asymmetry measurements bring new insight into the fundamental mechanisms of transverse spin asymmetries and Quantum Chromodynamical description of hadronic structure.

Keywords: Single Spin Asymmetries, BRAHMS, twist-3, Sivers
PACS: 13.85.Ni, 13.88+e, 12.38.Qk

INTRODUCTION

In the lowest-order QCD approximation, single transverse spin asymmetries (SSAs) in $p^\uparrow p$ ($\bar{p}^\uparrow p$) reactions at the energy regime where pQCD is applicable are expected to be negligibly small [1], whereas experimentally large SSAs have been observed at high x_F [2, 3]. Main theoretical focuses to account for the observed SSAs in the framework of QCD have been on the role of transverse momentum dependent (TMD) partonic effects in the structure of the initial transversely polarized nucleon [4] and the fragmentation process of a polarized quark into hadrons [5]. Higher twist effects (“twist-3”) arising from quark-gluon correlation effects beyond the conventional twist-2 distribution have been also considered as a possible origin of SSA [6, 7]. Recently, new measurements of SSAs have been available from semi-inclusive deep-inelastic scattering (SIDIS) [8, 9] and $p^\uparrow + p$ at RHIC providing more insight into the fundamental mechanisms of SSA as well as the relevant hadron structure [10, 11, 12]. SSA measurements in $p^\uparrow p$ at RHIC energy, $\sqrt{s} = 200$ GeV, are of particular interest because the next-to-leading-order (NLO) pQCD calculations [13] for the unpolarized (spin-averaged) meson cross-sections are successfully describing the data [10, 12]. At $\sqrt{s} \sim 20$ GeV where FNAL/E704 observed large SSAs, NLO pQCD calculations get almost an order of magnitude smaller than the similar measurements [14]. The two sets of data from FNAL and RHIC cover similar kinematic (x_F and p_T) range and the measurements show that SSAs for pions are energy independent to a first approximation. This might imply that the dominant mechanism responsible for the large SSAs at the two different energies are manifestation of two different phenomena. The newly available measurements from RHIC in the intermediate energy regime at $\sqrt{s} = 62.4$ GeV in $p^\uparrow p$ can uniquely provide an opportunity to clarify the pQCD contribution to SSAs and their energy dependences.

We present measurements of SSAs for π^\pm , K^\pm , p , and \bar{p} at forward rapidities covering high- x_F at $\sqrt{s} = 62.4$ GeV and also at $\sqrt{s} = 200$ GeV. A simultaneous description of

SSAs and the unpolarized cross-sections in wide kinematic range will be a crucial test for partonic pQCD description. In particular, flavor dependent SSA measurements allow more complete and stringent tests of theoretical models due to flavor dependence in parton distribution functions and fragmentation processes.

SSA MEASUREMENTS AT HIGH- x_F

The SSA is defined as a “left-right” asymmetry of produced particles from the hadronic scattering of transversely polarized protons off unpolarized protons. Experimentally the asymmetry can be obtained by flipping the spins of polarized protons, and is customary defined as analyzing power A_N :

$$A_N = \frac{1}{\mathcal{P}} \frac{(N^+ - \mathcal{L}N^-)}{(N^+ + \mathcal{L}N^-)}, \quad (1)$$

where \mathcal{P} is polarization of the beam, \mathcal{L} is the spin dependent relative luminosity ($\mathcal{L} = \mathcal{L}_+/\mathcal{L}_-$) and $N^{+(-)}$ is the number of detected particles with beam spin vector oriented up (down). The average polarization of the beam \mathcal{P} as determined from the on-line CNI measurements [5] is about 50% for Run-5 (200 GeV) and 60% for Run-6 (62.4 GeV) [15]. The systematic error on the A_N measurements is estimated to be 20% including uncertainties from the beam polarization ($\sim 18\%$). The systematic error represents mainly scaling uncertainties on the values of A_N .

The data presented here were collected with the BRAHMS detector system [16] in polarized $p + p$ collisions from RHIC-Run5 with recorded integrated luminosity corresponding to 2.4 pb^{-1} at $\sqrt{s} = 200 \text{ GeV}$ and from RHIC-Run6 with recorded integrated luminosity of 0.21 pb^{-1} at $\sqrt{s} = 62.4 \text{ GeV}$ [15]. The luminosity was measured using the “CC” counter which is a set of Cherenkov radiators placed symmetrically with respect to the nominal interaction point. The counters cover pseudo-rapidity (η) range in $3.26 < |\eta| < 5.25$, and are estimated to be sensitive to $\sim 70\%$ of the total inelastic $p + p$ cross-section of 41 mb at $\sqrt{s} = 200 \text{ GeV}$ and $\sim 33\%$ of 36 mb at 62.4 GeV . The Forward Spectrometer (FS) in BRAHMS has unique capability of measuring tracks in forward kinematic region ($\theta = 2.3^\circ - 15^\circ$) with good momentum resolution and particle identification (PID). The momentum (p) resolution at the maximum magnetic field setting of FS, which is the main setting used for the data taking at $\sqrt{s} = 200$, is estimated to be $\delta p/p \approx 0.0008p$ where p is in GeV. The PID separation of pions and kaons using Ring Image Cherenkov (RICH) [17] detector is up to $p \sim 35 \text{ GeV}/c$ and protons can be identified up to $45 \text{ GeV}/c$. The kinematic coverage of the data taken with BRAHMS-FS at 2.3° and 4° for $\sqrt{s} = 200 \text{ GeV}$ and at 2.3° and 3° for $\sqrt{s} = 62.4 \text{ GeV}$ as a function of p_T and x_F in Fig. 1. The narrow p_T - x_F correlated band at a given setting is due to the small aperture of the spectrometer.

RESULTS

The analyzing power A_N for charged pions, $A_N(\pi^+)$ and $A_N(\pi^-)$ at $\sqrt{s} = 200 \text{ GeV}$ as a function of x_F are shown in Fig. 2 for the two FS angle settings with p_T coverages

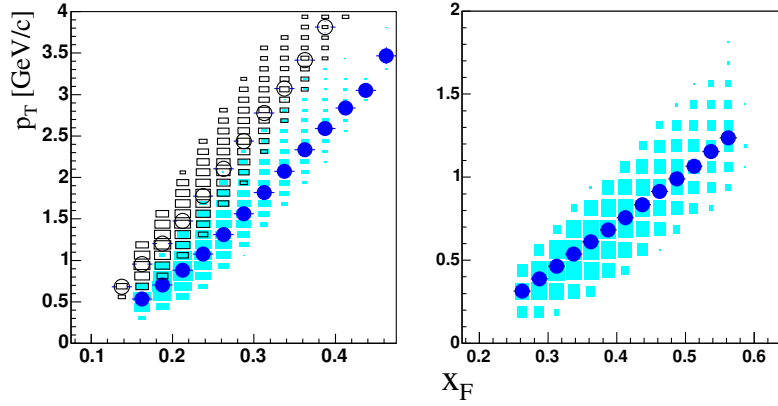


FIGURE 1. p_T vs. x_F for the data used in the SSA analysis at $\sqrt{s} = 200$ GeV (left Panel). The open symbols are for FS at 4° and closed boxes are at 2.3° at full field setting. At $\sqrt{s} = 62.4$ GeV (right panel), data from FS at 2.3° and 3° are combinedly used. Mean values of p_T at a given x_F value are displayed with circles.

shown in Fig. 1. The A_N values are positive for π^+ and negative for π^- decreasing with p_T . The asymmetries and their x_F -dependence are qualitatively in agreement with the measurements from E704/FNAL and also $A_N(\pi^0)$ measurements at RHIC [2, 10]. The $1/p_T$ dependence might indicate that A_N is in accordance with the expected power-suppressed nature of A_N [18]. Figure 2 compares $A_N(\pi)$ with a pQCD calculation in the range of $p_T > 1$ GeV/ c using “extended” twist-3 parton distributions [6] including the “non-derivative” contributions [18, 19, 20]. In this framework, two calculations from the model are compared with the data: two valence densities (u_v, d_v) in the ansatz with and without sea- and anti-quark contribution in the model fit. The calculations describe the data within the uncertainties. As the calculations shown in the figure, the dominant contribution to SSAs are from valence quarks and sea- and anti-quark contributions on SSAs are small that the current measurements are not able to quantitatively constrain the contribution. The data are also compared with Sivers mechanism which successfully describe FNAL/E704 A_N data. The calculations compared with the data use valence-like Sivers functions [21, 22] for u and d quarks with opposite sign. The fragmentation functions used are from the KKP parameterization [23], but the Kretzer fragmentation function [24] gives similar results. The calculations shown with dotted lines in the figure underestimate A_N for both p_T ranges, which indicates that TMD parton distributions are not sufficient to describe the SSA data at the energy. The Collins mechanism is not compared with the measurements since the Collins mechanism fails to describe $A_N(\pi^\pm)$ for the E704 data in particular at large- x_F [25].

The SSAs for charged kaons and protons as a function of x_F are shown in Fig. 3. Asymmetry for $K^+(u\bar{s})$ shows positive as A_N of $\pi^+(u\bar{d})$, which is expected if the asymmetry is mainly carried by valence quarks, but the measured positive SSAs of K^- and \bar{p} seem to contradict the naïve expectations [26] of valence quark dominance. In valence-like model (no Sivers effect from sea-quarks and/or gluons), non-zero positive $A_N(K^-)$ implies large non-leading fragmentation functions ($D_u^{K^-}, D_d^{K^-}$) and insignificant contribution from strange quarks. Twist-3 calculations also under-predict $A_N(K^-)$ due to the

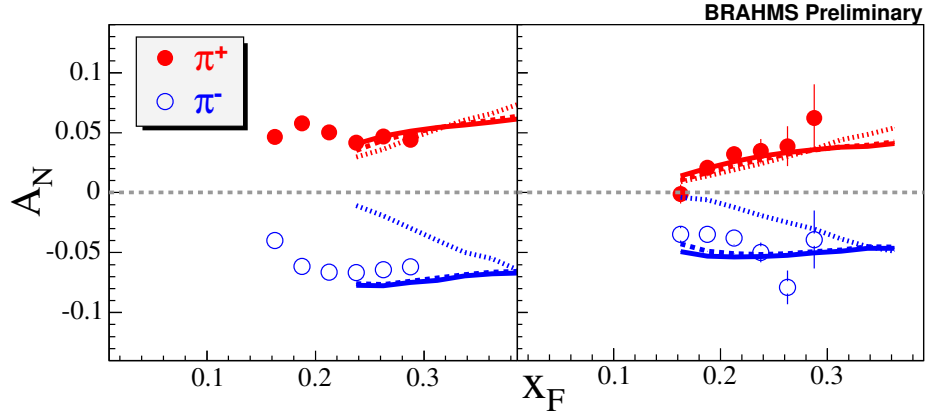


FIGURE 2. A_N vs. x_F for pions. Solid symbols are for $A_N(\pi^+)$ and open symbols are for $A_N(\pi^-)$ measured using FS at 2.3° (left panel) and 4° (right panel). The curves are from the twist-3 calculations with (line) and without (broken) sea- and anti-quark contribution. Prediction from Sivers effect is shown with dotted lines. Only statistical errors are shown where larger than symbols.

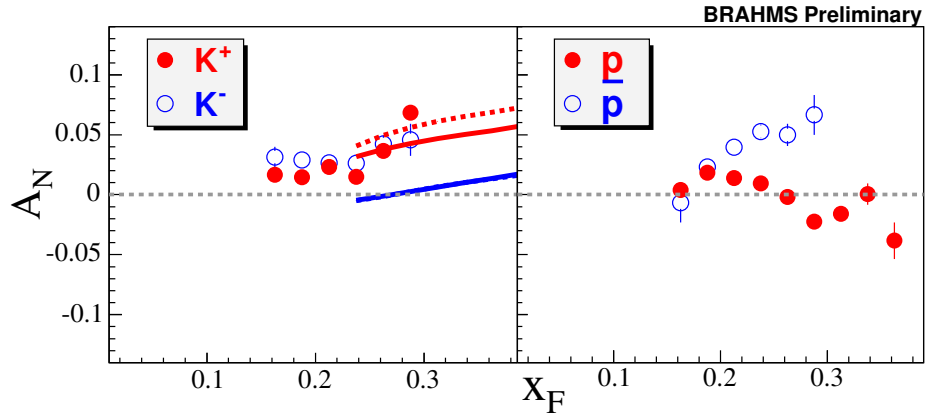


FIGURE 3. A_N vs x_F for K^+ , K^- , p and \bar{p} at $\sqrt{s} = 200$ GeV. measured with FS at 2.3° . The curves are from the twist-3 calculations with (line) and without (broken) sea- and anti-quark contribution. Only statistical errors are shown where larger than symbols.

small contribution of sea and strange-quark contribution to A_N in the model. In Fig. 3, protons show no significant asymmetries compared to anti-protons, but require more understanding of their production mechanism to theoretically describe the behavior because a significant fraction of the protons might still be related to the polarized beam fragments under the constraint of baryon conservation at this kinematic range.

The analyzing power A_N for charged pions in $p^\uparrow + p$ collisions at $\sqrt{s} = 62.4$ GeV as a function of x_F are shown in Fig. 4 with p_T coverages as shown in Fig. 1. The measured A_N values show strong dependence in x_F reaching large asymmetries reaching up to $\sim 40\%$ at $x_F \sim 0.6$.

In $p^\uparrow + p$ collisions, SSAs at $x_F < 0$ probe the kinematics of the sea (gluon) region of p^\uparrow at small- x and the valence region of p . The measured insignificant A_N in $x_F < 0$, where $\hat{u} \rightarrow 0$, indicate that A_N is dominated by the process where \hat{t} is small, and shows

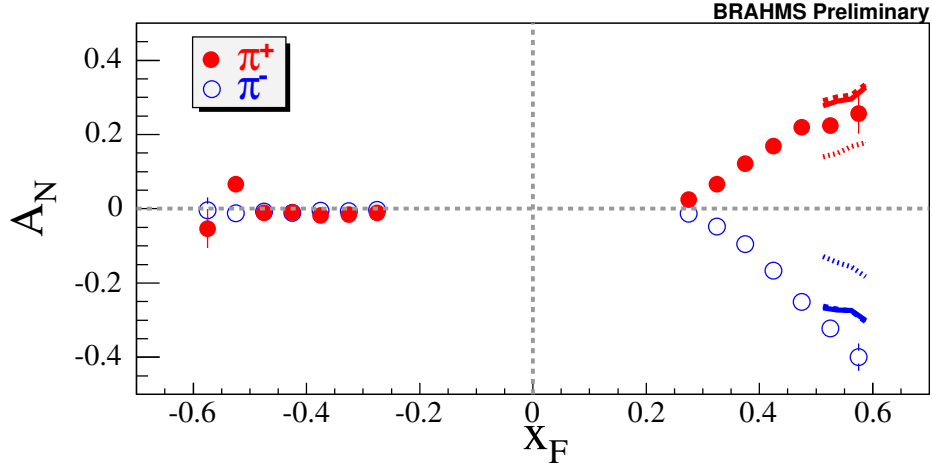


FIGURE 4. A_N vs. x_F for π^+ and π^- at $\sqrt{s} = 62$ GeV for positive and negative x_F . Solid symbols are for π^+ and open symbols are for π^- measured in FS at 2.3° and 3° . The curves are from the twist-3 calculations with (line) and without (broken) sea- and anti-quark contribution. Predictions from the Siverson function calculations is shown as dotted lines. Only statistical errors are shown where larger than symbols.

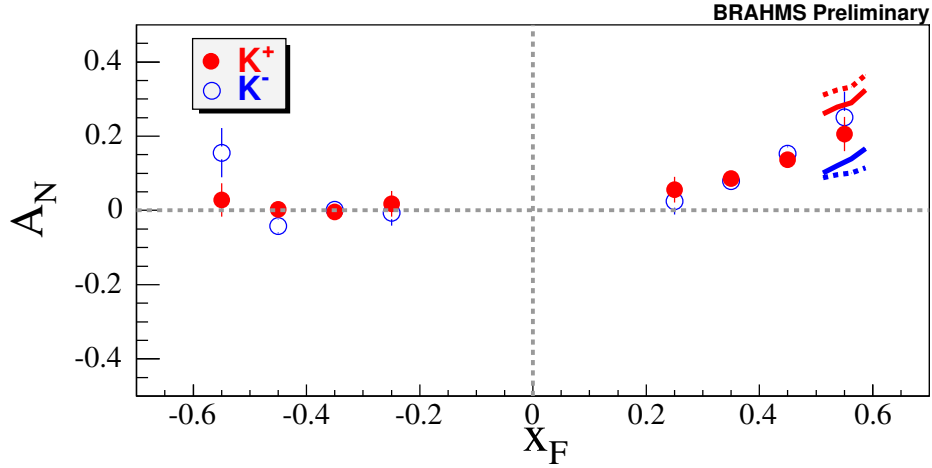


FIGURE 5. $A_N(K^+)$ and $A_N(K^-)$ vs. x_F at $\sqrt{s} = 62$ GeV for positive and negative x_F . Solid symbols are for K^+ and open symbols are for K^- . The curves are from the twist-3 calculations with (line) and without (broken) sea- and anti-quark contribution. Errors are statistical only.

no significant contribution to A_N from processes where gq scattering is enhanced.

Compared with twist-3 calculations for $p_T > 1$ GeV/c, A_N for π^+ and π^- are in agreement qualitatively while Siverson effect under-predicts especially for π^- . Similarly as for the 200 GeV data, strangeness asymmetries at 62.2 GeV, $A_N(K^-)$ needs an extra or a different mechanism to account for positively non-zero $A_N(K^-)$ at similar level of $A_N(K^+)$ as shown in Fig. 5.

SUMMARY

In summary, BRAHMS has measured SSAs for inclusive identified charged hadron production at forward rapidities in $p^\uparrow+p$ at $\sqrt{s} = 200$ GeV and 62.4 GeV. A twist-3 pQCD model of A_N describes x_F dependent $A_N(\pi)$ and their energy dependence at high p_T ($p_T > 1$ GeV/c) where the calculations are applicable, but it's challenging for pQCD models consistently describe spin-averaged cross section at lower energies.

Measurements of A_N for kaons and protons suggest the manifestation of non-pQCD phenomena and/or a call for more theoretical modeling with good understanding of the fragmentation processes. The energy and flavor dependent SSA measurements of identified hadrons allow more complete and stringent tests of theoretical models of partonic dynamics in the RHIC energy regime.

ACKNOWLEDGMENTS

We thank Feng Yuan and Umberto D'Alesio for providing us with their calculations shown in this contribution. This work is supported by the Division of Nuclear Physics of the Office of Science of the U.S. Department of energy under contract DE-AC02-98-CH10886.

REFERENCES

1. G.L. Kane, J. Pumplin and W. Repko, *Phys. Rev. Lett.* **41** 1689 (1978).
2. D.L. Adams *et al.* (E704 Collaboration), *Phys. Lett.* **B264** 462 (1991).
3. A. Bravar *et al.* (E704 Collaboration), *Phys. Rev. Lett.* **77** 2626 (1996).
4. D. Sivers, *Phys. Rev.* **D41** 83 (1990).
5. J.C. Collins, *Nucl. Phys.* **B396** 161 (1993).
6. J. Qiu and G. Sterman, *Phys. Rev.* **D59** 014004 (1999).
7. For a review, see J. Kodaira and K. Tanaka, *Prog. Theor. Phys.* **101** 191 (1999).
8. A. Airapetian *et al.*, (HERMES Collaboration) *Phys. Rev. Lett.* **94** 012002 (2005).
9. V.Y. Alexakhin *et al.*, (COMPASS Collaboration) *Phys. Rev. Lett.* **94** 202002 (2005).
10. J. Adams *et al.* (STAR Collaboration), *Phys. Rev. Lett.* **92** 171801 (2004).
11. F. Videbaek (BRAHMS Collaboration) AIP Conf. Proc. **792** 993 (2005).
12. J.H. Lee (BRAHMS Collaboration) in Proceedings of XIV International Workshop on Deep Inelastic Scattering (DIS06), Tsukuba, Japan (2006), to be published.
13. B. Jager *et al.*, *Phys. Rev.* **D67** 054005 (2003).
14. C. Bourrely and J. Soffer, *Eur. Phys. J.* **C36** 371 (2004).
15. M. Bai, these proceedings.
16. M. Adamczyk *et al.* (BRAHMS Collaboration), *Nucl. Instr. Meth.* **A499** 437 (2003).
17. R. Debbé *et al.*, *Nucl. Instr. Meth.* **A570** 216 (2007).
18. C. Kouvaris *et al.*, *Phys. Rev.* **D74** 1104013 (2006).
19. W. Vogelsang, these proceedings.
20. The calculations were provided by F. Yuan.
21. U. D'Alesio and F. Murgia, *Phys. Rev.* **D70** 074009 (2004), these proceedings.
22. The calculations were provided by U. D'Alesio.
23. B.A. Kniehl *et al.*, *Nucl. Phys.* **B597** 337 (2001).
24. B.A. Kretzer, *Phys. Rev.* **D62** 054001 (2000).
25. M. Anselmino *et al.*, *Phys. Rev.* **D71** 014002 (2005).
26. M. Anselmino *et al.*, *Phys. Lett.* **B442** 470 (1998).